DC AND RF CHARACTERIZATION OF n-GaN SCHOTTKY DIODE FOR MICROWAVE APPLICATION

by

TARIQ MUNIR

Thesis submitted in fulfillment of the requirements
for the degree of
Doctor of Philosophy

January 2011

ACKNOWLEDGEMENTS

I am grateful to Allah, our Lord and Cherisher, The Merciful and The Sustainer, for His mercy, love, and strength granted for me so that I have been able to finish this thesis. I would like to express my deepest gratitude to my supervisor, Assoc. Prof. Azlan Abdul Aziz, for his guidance, cooperation, valuable discussions and dedicated support throughout the course of this project. I also admire his patience and humble behavior during research discussion and practical life. I would like to sincerely thanks to my co-supervisor Prof. Mat Johar Abdullah and Assoc. Prof. Mohd Fadzil Ain for their detailed and constructive comments, and for their important support throughout this work.

I would like to thanks Dean Prof. Zainuriah Hassan, Prof. Kamarulazizi Ibrahim and Assoc.Prof. Roslan Hashim for their efforts in advancement of NOR lab equipments and simulation programme. I would like to take this opportunity to thanks to Nor Lab staffs; Mr Mokhtar, Mr Jamil, Mr Nizzam, Mr Azha, Mr Abdul Mutalib and Miss Ee Bee Choo for their generous help and technical support offered during my laboratorial work.

I owe my loving thanks to my dearest wife, Dr. Irsa Tariq, for her caring, loving, encouragement, patience and understanding. She helped me to complete my thesis. A special word of thanks goes to my elder brother Dr. Iqbal Munir, his wife Dr. Saima and niece mano, my son Muhammad Ali &daughter Sara for their loving support. I wish to thanks my parents Mr and Mrs Munir Hussain for their prays, brother advocate Imran Munir and my loving sister for their care and love. They bore me, raised me, supported me, taught me, and loved me.

Finally but most importantly, I wish to acknowledge Malaysian Technical Cooperation Programme for financial assistance throughout this study.

TABLE OF CONTENTS

	Page
ACKNOWLEDGEMENTS………………………………………………..	**ii**
TABLE OF CONTENTS……………………………………………...	**iii**
LIST OF TABLES …………………………………………………	**ix**
LIST OF FIGURES ………………………………………………..	**x**
LIST OF SYMBOLS ………………………………………………	**xvi**
LIST OF MAJOR ABBREVIATIONS ………………………………..	**xix**
ABSTRAK ………………………………………………………….	**xx**
ABSTRACT ………………………………………………………...	**xxiii**

CHAPTER 1 : INTRODUCTION **1**

1.1	Introduction to Schottky diode ……………………………………	1
1.2	Ideal material properties for high power and high frequency Application …………………………………………………….	4
1.3	Issues in GaN Schottky diode ……………………………………	6
1.4	Research objective ………………………………………………	8
1.5	Thesis organization ……………………………………………….	10

CHAPTER 2 : OVERVIEW OF GaN SCHOTTKY DIODE **12**

2.0	Introduction …………………………………………………..	12
2.1	Metal contact technology ………………………………………	12
	2.1.1 Energy band diagram of metal/semiconductor and Schottky barrier formation ………………………………………	14
	2.1.2 Conduction mechanism for metal/semiconductor contacts …	17
	2.1.3 Current conduction mechanism in metal/semiconductor ….. .	18
2.2	Metal-GaN contact technology ……………………………………	20
2.3	Ohmic contact to GaN ……………………………………….	21
	2.3.1 n-type conduction layer after thermal annealing …………..	23
2.4	Schottky contacts to GaN ………………………………………	24

2.4.1 Thermal behavior ………………………………………….. 27
2.4.2 p-type conduction layer after thermal annealing ………….. 29
2.4.3 Thermal annealing effect on Schottky barrier height and ideality factor ………………………………………... 30
2.5 Schottky contact area ………………………………………... 31
2.5.1 Schottky diode equivalent circuit and key factor limiting maximum frequency ………………………………………… 32
a. Series resistance (Rs) ………………………………… 33
b. Junction capacitance (C_J) ……………………………… 34
c. Figure of Merit ……………………………………….. 35
2.6 Edge termination technique …………………………………... 36

CHAPTER 3: DC AND RF CHARACTERIZATION TECHNIQUE 38

3.1 DC parameter measurement ………………………………… 38
3.1.1 Current-voltage measurements (I-V) …………………… 38
a. Barrier height ………………………………………… 41
b. Ideality factor ………………………………………… 41
c. Series resistance ……………………………………... 42
3.1.2 Capacitance- voltage measurement (C-V) ……………… 42
a. Theory ……………………………………………….. 42
3.2 RF parameter measurement ………………………………… 45
3.2.1 S-parameter characterization …………………………… 46
a. Two-port networks …………………………………… 48
b. Transmission line theory ……………………………… 50
c. Impedance matching ………………………………… 51
3.3 Filter characteristics ………………………………………... 53
3.3.1 Filter circuit …………………………………………….. 53
a. Low pass filter ……………………………………… 54
b. High-pass filters …………………………………... 55
3.3.2 Resonant filters ……………………………………… 56
a. LC ("tank") circuits …………………………………… 56
b. Resonant frequency …………………………………….. 58

CHAPTER 4: SIMULATION TOOLS AND MODELS 60

4.0 Introduction …………… ………………………………………… 60
4.1 ATLAS Device simulator …………………………………... 60
4.2 GaN Schottky diode simulation procedure ………………….. 62
4.3 Structure specification ……………………………………….. 62
4.3.1 Mesh generation ……………………………………….. 62
4.3.2 Region and Electrode specification ………………….. 63
4.3.3 Doping profile ………………………………………. 64
4.4 Material models specification …………………………….. 64
4.5 Materials statement ……………………………………... 64
4.5.1 Schottky contact ……………………………… 65
4.6 Models statement ……………………………………….. 65
4.6.1 Carrier Statistics Model ………………………………… 66
a. Fermi statistics ……………………………………... 66
b. Effective density of states ……………………………. 66
c. Energy bandgap ………………………………….. 67
d. Bandgap narrowing ……………………………... 67
e. Incomplete ionization model ……………………… 68
4.6.2. Mobility model …………. ……………………………… 68
a. Low field mobility 69
b. High field effect mobility …………………………… 70
4.6.3. Carrier Generation -Recombination model ………………. 71
a. Shockley –Read –Hall (SRH) recombination ……… 71
b. Auger recombination …………………………………... 72
c. Impact ionization model …………………………………… 73
d. Selberherr's impact ionization model ……………….. 74
4.7 Numerical method selection …………………………………….. 74
4.8 Solution specification ………..…………………………………….. 75
4.9 DC characteristics ……………………………………………. 76
4.9.1 Forward bias (I-V) characteristics ………………………. 76

4.9.2 Reverse bias (I-V) characteristics ………. ………………… 76
4.9.3 AC characteristics: (C-V) Characteristics …………………. 77
4.9.4 Simulation at elevated temperature …….. ………………….. 78
4.10 RF characteristics …………..……………………………………. 78
4.10.1 AC analysis with S-parameter ……….……………………… 78
4.10.2 Parasitic parameter ………… …………………………….. 79
4.11 Results analysis ………….. ……………………………………… 79
4.11.1 Log files …………... ……………………………………... 80
4.11.2 Solution files ……….……………………………………... 80
4.11.3 Invoking Tony Plot ……………………………………... 80
4.11.4 ATLAS extract ……………. ……………………………… 80
4.12 GaN Schottky diode structure and geometry …………………….. 81

CHAPTER 5: GaN SCHOTTKY DIODE DC AND RF CHARACTERISTICS: SIMULATION APPROACH **83**

5.0 Introduction ……….……………………………………………….. 83
5.1 Study of metal contact …..………………………………………. 83
5.1.1 Electrical characteristics ………… ………………………. 85
5.1.2 Summary ………………… ……………………………….. 88
5.2 Thermal behavior ………………………………………………… 89
5.2.1 Electrical characteristics ………...………………………… 89
5.2.2 RF characteristics …………..…………………………….. 94
5.2.3 Summary ………….……………………………………… 96
5.3 Schottky contact area ………. …………………………………… 97
5.3.1 Electrical characteristics …….……………………………. 97
5.3.2 RF characteristics ……….………………………………… 100
5.3.3 Summary ………………………………………………… 102
5.4 Edge termination technique ……………………………………... 103
5.4.1 Electrical characteristics ………………………………... 104
5.4.2 Summary …………………..……………………………… 108

CHAPTER 6: SCHOTTKY DIODE FABRICATION PROCESSES **109**

6.1 Wafer cleaning ………………………………………………... 109
6.2 Photolithographic ground-signal-ground GSG mask ………….. 109
6.3 Photolithography …………………………………………… 111
6.4 Mesa etching …………………………………………........ 112
6.4.1 Mesa RIE ………………...………………………………... 114
6.5 Metallization ………………………………………………….. 115
6.5.1 Thermal evaporation …….………………………………. 115
6.5.2 D.C sputtering …………………………………………… 116
6.6 Lift-off process ……………….……………………………… 117
6.7 Thermal annealing processes ………………………………….. 118
6.7.1 Conventional furnace ………………………………. 119
6.8 Mesa mask fabrication process ……………………………….. 121
6.9 Mesa mask step by step fabrication process ………………….. 122

CHAPTER 7: RESULTS AND DISCUSSION **123**

7.0 Introduction …………………………………………………… 123
7.1 Metal contact study ……………….…………………………. 123
7.2 Ohmic contacts on n-GaN ……………………………………… 123
7.2.1 Electrical characteristics…………………………………… 124
7.2.2 Capacitance-voltage ……………………………………... 125
7.2.3 SEM analysis.. 126
7.2.4 XRD results…………………………………………………. 127
7.2.5 Analysis on ohmic contact………………………………….. 129
7.3 Schottky contacts on n-GaN …………………………………….. 130
7.3.1 Electrical characteristics ……………………………………. 131
7.3.2 SEM analysis ……………………………………………….. 133
7.3.3 XRD results ………………………………………………... 136
7.3.4 Schottky contact analysis ………………………………….. 139
7.3.5 RF analysis ……………………………………………….. 142

7.4 Comparative study of Pt/Pd, Pt/Ti and Pt/Ni bilayer Schottky metal contact ……………… 145
7.4.1 Electrical characteristics ……………… 146
7.4.2 SEM analysis ……………… 148
7.4.3 XRD results ……………… 149
7.4.4 Bilayer Schottky contact analysis ……………… 152
7.4.5 RF characteristics ……………… 153
7.5 Summary ……………… 158
7.6 De-embedding technique ……………… 159

CHAPTER 8: CONCLUSION AND FUTURE STUDIES **161**

8.1 Conclusion ……………… 161
8.1.1 Metal contact study ……………… 161
8.1.2 Thermal behavior ……………… 163
8.1.3 Schottky contact area ……………… 164
8.1.4 Edge termination ……………… 164
8.2 Future Studies ……………… 165
REFERENCES ……………… 169
APPENDICES ……………… 183
Appendix 1:Simulation profile run in ATLAS ……………… 183
Appendix 2:GaN Schottky diode simulation parameters ……………… 187
Appendix 3:Tools and characterization ……………… 188
Appendix 4:De-embedding technique ……………… 198
LIST OF PUBLICATIONS……………… 199

LIST OF TABLES

		Page
Table 1.1	Material properties of common semiconductors. (Golio, 2003)	6
Table1.2	GaN properties for high power and high frequency. (Borges. 2001)	6
Table 2.1	Electrical Nature of Ideal MS contacts. (Pierret, 1996)	13
Table 2.2	Summary of measured parameter. (Schmitz *et al.* 1996)	27
Table. 4.1	GaN low-field mobility at room temperature. (Mnatsakanov *et al.* 2003)	70
Table. 4.2	Parameters for calculating the R_{SRH} and R_{Au} of GaN.	73
Table. 4.3	Ionization coefficient of GaN. (Baik *et al.* 2003)	74
Table 5.1	Summary of simulated (I-V) parameters for Pt, Ni, Au, Ti, and Al on n-GaN.	88
Table 5.2	Simulated Schottky contact length (I-V) parameter.	99
Table 5.3	Simulated edge termination (I-V) parameters.	104
Table 6.1	The steps in lithography process. (Levinson *et al.* 2001).	112
Table 6.2	GaN mesa RIE recipe.	114
Table 6.3	n-GaN samples metal contacts and thermal treatment.	120
Table 7.1	Measured thermally annealed (I-V) parameters of Pt, Pd and Ni Schottky metal contact on n-GaN.	133
Table 7.2	Measured thermally annealed (I-V) parameters of Pt/Pd, Pt/Ni and Pt/Ti Schottky metal contact on n-GaN.	148

LIST OF FIGURES

		Page
Figure 1.1	(a) Point contact diode. (b) Planar Schottky barrier diode. (c) Problems in Schottky diode. (d) Edge-termination Schottky diode. (Fnrf, 2004 & Adrio communication, 2005)	4
Figure 2.1	Characteristics of (a) rectifying, (b) linear or ohmic I-V.	13
Figure 2.2	Energy band diagrams for an ideal metal/n-type semiconductor contact. (Sheng, 2005)	14
Figure 2.3	Conduction mechanism for metal/n-semiconductor contacts as a function of the barrier height and width.	18
Figure 2.4	Energy band diagrams and current components for Schottky barrier diode under (a) Zero bias (b) forward bias (c) reverse bias. (Sheng, 2005)	19
Figure 2.5	Ohmic behavior of Al/Ti contact on non-preannealed n-GaN samples as a function of annealing. (Liu and Lau, 1998)	23
Figure 2.6:	Schematic illustration of the n-GaN substrate annealed at 700°C.	24
Figure 2.7	Reported barrier height of metals to n-GaN as a function of their work function. (Liu and Lau, 1998)	26
Figure. 2.8	Energy band diagrams at the metal/GaN interface a) with contamination layer, and b) without contamination layer.	31
Figure.2.9	(a) Cross section of Schottky barrier diode (b) Equivalent circuit of Schottky diode. (Terri, 2002)	32
Figure.2.10	Current distribution at high frequency in dot-matrix diode. (Terri, 2002)	34
Figure 2.11	Schottky diode structures: (a) with field plate edge termination. (Tarplee *et al.* 2001) (b) Ramp oxide termination structure. (Badila and Brezeanu, 1995)	37
Figure 3.1	(a) Semi-logarithmic I-V plot for Schottky diode. (Shabbir, 1998) (b) Forward bias Schottky diode parameter measurement.	40

Figure 3.2	Typical C-V curve showing Accumulation, Depletion and Inversion region.	43
Figure 3.3	Charges in a Metal-Semiconductor interface under: a) accumulation b) depletion c) inversion conditions.	44
Figure 3.4	Light interaction through lens. (Sischka, 2002)	47
Figure 3.5	Two-port network. (Anderson, 1996)	48
Figure 3.6	Simplified diagram of impedance matching network.(Smith, 1931)	52
Figure 3.7	Low pass filter circuit and frequency response. (Kuphaldt, 2007)	54
Figure 3.8	High pass filter circuit and frequency response. (Kuphaldt, 2007)	55
Figure 3.9	Series LC resonant filter (a) Series (LC) tank circuit (b) Frequency response. (Kuphaldt, 2007)	57
Figure 3.10	Parallel LC resonant filter (a) Parallel tank circuit (b) Frequency response. (Kuphaldt, 2007)	58
Figure 4.1	Silvaco Simulation Tool	60
Figure 4.2	ATLAS tool flow.	61
Figure 4.3	(a)Vertical (b) Lateral GaN Schottky diode structure. (Jihyun *et al.* 2005)	82
Figure. 5.1	Simulated n-GaN Schottky structure for metal contact.	84
Figure.5.2	(I-V) characteristics of Pt metal contact for epilayer thickness and doping density variation. (a) Forward bias for different epilayer thickness (b)Series resistance vs epilayer thickness (c) Reverse voltage vs epilayer thickness (d) Reverse voltage vs epilayer carrier concentration.	84
Figure 5.3	Forward Log I vs V characteristics of different metal contact on n-GaN.	86
Figure 5.4	Relation of ideal and simulated barrier height to different metal work function with n-GaN.	87
Figure 5.5	Reverse (I-V) characteristics of different metal contacts on n-GaN.	88
Figure 5.6	Simulated n-GaN Schottky diode structure for thermal behavior.	89

Figure 5.7	Temperature dependence forward bias (I-V) characteristics of GaN Schottky diode.	90
Figure 5.8	Barrier height and ideality factor with temperature variation.	90
Figure 5.9	Series-resistance with temperature variation.	91
Figure 5.10	Temperature dependence reverse bias I-V characteristics of GaN Schottky diode.	92
Figure 5.11	Fermi level variation with temperature. (Benden *et al.* 1999)	93
Figure 5.12	Temperature dependence Capacitance - Voltage characteristics of GaN Schottky diode.	94
Figure 5.13	Input return loss (S_{11}dB) of GaN at higher temperature.	95
Figure 5.14	Insertion loss (S_{21}dB) of GaN Schottky diode with temperature variation.	96
Figure 5.15	Simulated lateral Schottky diode structure for Schottky contact area.	97
Figure 5.16	Forward bias I-V characteristics of GaN Schottky diode at different Schottky contact length.	98
Figure 5.17	Reverse bias I-V characteristics of GaN Schottky diode at different Schottky contact length.	99
Figure 5.18	Capacitance - Voltage characteristics of GaN Schottky diode at different Schottky contact length.	100
Figure 5.19	Input return loss (S_{11} dB) of GaN Schottky diode at different Schottky contact length.	101
Figure 5.20	Insertion loss (S_{21} dB) of GaN Schottky diode at different Schottky contact length.	102
Figure. 5.21	Simulated edge termination structure (a) Metal overlap on oxide layer. (b) Ramp oxide edge termination.	103
Figure 5.22	Forward I-V characteristic, indicating increasing resistance as oxide thickness used under metal overlap termination increases.	104

Figure 5.23	Forward current density (a) without edge termination (b) with metal overlaps edge termination of n-GaN Schottky diode.	105
Figure 5.24	Forward bias I-V characteristics at different field plate overlap length(x_0).	106
Figure 5.25	Forward bias I-V characteristics of oxide Vs ramped oxide of n-GaN Schottky diodes.	107
Figure 5.26	Reverse bias I-V characteristics at different oxide thickness of n-GaN Schottky diodes.	108
Figure 6.1	a) Microwave probe types b) Microwave pad pattern for each measurement port.	110
Figure 6.2	Fabricated GSG pad pattern (a) 400×400μm^2 mesa (b) 400×100μm De-embedding mesa (c), (d), (e) (400×100μm^2) GSG ohmic and Schottky contact, (f) (100×100μm^2) Schottky contact GSG. Circular and triangle structure serve as alignment maker.	111
Figure 6.3	a) Simplified diagram of plasma RIE system b) Equipment Plasma RIE system used in lab.	113
Figure 6.4	n-GaN samples under plasma RIE etch.	114
Figure 6.5	(a) Setup of thermal evaporator. (b) Actual picture of thermal evaporator.	116
Figure 6.6	(a) Setup of D.C sputtering system. (b) Actual picture of D.C sputtering system.	117
Figure 6.7	(a) Setup of tube furnace for thermal annealing. (b) Actual picture of the thermal annealing tube furnace.	119
Figure 6.8	Mesa mask fabrication process.	121
Figure 6.9	Flowchart of mesa mask (GSG) step by step fabrication process.	122
Figure 7.1	Al/Ti as ohmic contact on n-GaN diode structure.	124
Figure 7.2	(I-V) Characteristics of Al/Ti on n-GaN annealed from 400°C to 900°C for 20 s in N_2	125

Figure 7.3	(C-V) Characteristics of Al/Ti annealed from 400°C to 900°C for 20 s in N_2.	126
Figure 7.4	SEM images of Al/Ti ohmic contact on n-GaN at (a) 400ºC (b) 500ºC (c) 700ºC and (d) 900ºC.	127
Figure 7.5	XRD spectra of Al/Ti (a) as deposited (b) 500°C and (c) 700°C for 20 s in N_2.	128
Figure 7.6	Cross section of n-GaN Schottky diode structure showing ohmic and Schottky contact placement with two grounding points (G) for RF measurement.	130
Figure 7.7	(I-V) characteristics of thermally annealed Pt, Pd and Ni on n-GaN from 400ºC to 600ºC for 10min.	131
Figure 7.8	SEM images of Pt Schottky contact annealed from 400ºC to 600ºC.	134
Figure 7.9	SEM images of Ni Schottky contact annealed from 400ºC to 600ºC.	135
Figure 7.10	SEM images of Pd Schottky contact annealed from 400ºC to 600ºC.	135
Figure. 7.11	XRD spectra of (a), (b), (C) Pt annealed at 400ºC, 500ºC and 600ºC.	136
Figure. 7.12	XRD spectra of (a), (b), (C) Pd annealed at 400ºC, 500ºC and 600ºC.	137
Figure. 7.13	XRD spectra of (a), (b), (C) Ni annealed at 400 ºC, 500ºC and 600ºC.	138
Figure 7.14	Insertion loss (S_{21}dB) of Pt, Ni and Pd Schottky metal contact at room temperature.	143
Figure. 7.15	Insertion loss (S_{21} dB) of Pt Schottky metal contact on n-GaN by simulation and fabrication approach.	144
Figure 7.16	Cross section of n-GaN Schottky diode structure showing ohmic and Schottky contact placement with two grounding points (G) for RF measurement.	145

Figure. 7.17	Temperature variation (I-V) characteristics of Pt/Pd, Pt/Ni and Pt/Ti Schottky metal contact on n-GaN.	146
Figure 7.18	(I-V) characteristics of single layer Pt and bilayer Pt/Pd Schottky metal contact on n-GaN.	147
Figure 7.19	SEM image of (a), (b,) (c), Pt/Pd and (d), (e), (f) Pt/Ni and (g), (h), (i) Pt/Ti annealing at 400ºC, 600ºC and 800ºC under N_2 ambient for 10 min.	149
Figure. 7.20	XRD spectra of (a), (b) Pt/Pd Schottky metal contact on n-GaN as deposit and annealing at 600ºC.	150
Figure. 7.21	XRD spectra of (a), (b) Pt/Ni Schottky metal contact on n-GaN as deposit and at 600ºC.	151
Figure. 7.22	XRD spectra of (a), (b) Pt/Ti Schottky metal contact on n-GaN as deposit and at 600ºC.	151
Figure 7.23	Thermal insertion losses (S_{21} dB) of (a) Pt/Pd (b) Pt/Ni and (c) Pt/Ti bilayer Schottky metal contact annealed from 400ºC to 800ºC on n-GaN.	156
Figure 7.24	Insertion loss (S_{21} dB) of fabricated bilayer Pt/Pd and Pt Schottky metal contact, and simulated Pt Schottky metal contact on n-GaN at room temperature.	157
Figure 7.25	Parasitic losses of Schottky contact area $50\times100\mu m^2$ and $400\times100 \mu m^2$ before and after de-embedding.	160

LIST OF SYMBOLS

Roman Symbols*:*

A	Area
A**	Richardson's constant
C_j	Junction capacitance
E_{cr}	Critical field
Ev	Valence band
Ec	Conduction band
Eg	Semiconductor bandgap
E_b	Breakdown field
I	Current
I_o	Saturation current
J_{sm}	Current density from semiconductor to metal
J_{ms}	Current density from metal to semiconductor
J_0	Saturation current density
K	Boltzmann's constant
m_o	Electron mass
m^*	Effective mass
m_n	Electron effective mass
m_p	Hole effective mass
N_D	Donor concentration
N_A	Acceptor concentration
N^-_A	Acceptor impurity
N^+_D	Ionized donor impurity
N_C	Conduction band
N_V	Valence band
Ns	Sheet concentration
N	Carrier concentration
Q	Electron charge
Rs	Series resistance
R_{Au}	Auger recombination
R_{SRH}	Shockley-Read-Hall recombination

R_s	Sheet resistance
R_j	Junction resistance
S_{11}	Input reflection coefficient
S_{22}	Output reflection coefficient
S_{21}	Forward transmission (insertion) gain
S_{12}	Reverse transmission (insertion) gain
t_{epi}	Epilayer thickness
V_F	Forward voltage
V_R	Reverse voltage
V_b	Built in charge
V_{BR}	Breakdown voltage
v_d	Drif velocity
W_D	Depletion layer width
E_D	Width between donor level and conduction band
X_{dep}	Depletion width
Z_S	Source impedance
Z_L	Load impedance

Greek Symbols:

α	Absorption coefficient
ε	Dielectric permittivity
ε_o	Absolute dielectric constant
ε_r	Relative dielectric constant
ε_s	Dielectric permittivity
σ	Conductivity
η	Ideality factor
Φ_B	Schottky barrier height
ϕ_M	Metal work function
ϕ_S	Semiconductor work function
φ_{Bn}	Potential barrier
ρ	Resistivity
ρ_c	Specific contact resistivity (Ωcm^2)
τ_n	Lifetime of electrons

τ_p	Lifetime of holes
Γ	Ratio of the reflected wave to the incident wave
μ_n	Electron mobility
μ_p	Hole mobility
ω	Photon frequency
λ	Wavelength
χ	Semiconductor electron affinity

LIST OF MAJOR ABBREVIATIONS

AFM	Atomic force microscopy
ASCII	American Standard Code for Information Interchange
ATUs	Antenna tuners
BFM	Baliga's figure of merit
C-V	Capacitance-Voltage
C.F	Correction factors
CFOM	Combined figure-of-merit
DC	Direct current
DUT	Diode under test
EMI	Electromagnetic interference
EDX	Energy dispersive X-ray
GaN	Gallium nitride
GaAs	Gallium Arsenide
GSG	Ground-signal-ground
GND	Ground
ICP	Inductively coupled plasma
I-V	Current-Voltage
MBE	Molecular Beam Epitaxial
MS	Metal Semiconductor
MESFETs	Metal-Semiconductor Field Effect Transistor
Pt	Platinum
Pd	Palladium
RF	Radio Frequency
RIE	Reactive ion etching
RL_{out}	Output return loss
SP	Scattering parameters
SBH	Schottky barrier height
SEM	Scanning electron microscope
SUT	Sample under test
TiN	Titanium nitride
WBG	wide-bandgap semiconductor
XRD	X-ray diffraction

PENCIRIAN DC DAN RF DIOD SCHOTTKY n-GaN UNTUK APLIKASI GELOMBANG MIKRO

ABSTRAK

Galium nitrida adalah bahan semikonduktor jurang jalur lebar yang berpotensi untuk aplikasi peranti pada kuasa, suhu dan frekuensi tinggi. Namun begitu, ada beberapa faktor yang menghadkan prestasi bahan untuk peranti tersebut. Antara faktor yang kritikal dan paling penting ialah kebocoran arus pincang belakang, kerintangan parasitik, kapasitan simpang dan kestabilan terma, yang menghalang peningkatan prestasi dalam cirian arus terus (DC) dan frekuensi radio (*RF*) bahan Galium nitrida. Untuk mengatasi kelemahan tersebut, kajian terhadap pengaruh sentuhan logam, luas sentuhan, sifat terma dan penamatan tebing berkaitan ciri *DC* dan *RF* diod schottky n-GaN telah dilakukan melalui kaedah simulasi dan eksperimentasi peranti.

Untuk kajian sentuhan logam, simulasi dan fabrikasi diod schottky n-GaN dimulai dengan menggunakan pelbagai jenis logam tunggal schottky (Platinum (Pt), Nikel (Ni), dan Paladium (Pd)) dan logam dwi-lapisan (Pt/Pd, Pt/Ni, Platinum/ Titanium (Pt/Ti)) di sepuhlindap pada suhu bilik sehingga suhu 800°C manakala Al/Ti sebagai sentuhan ohmik yang di sepuhlindap dari suhu bilik sehingga suhu 900°C bagi mengkaji kesan kebocoran arus pincang belakang, kestabilan terma dan kerugian penyisipan dengan menggunakan beberapa kaedah seperti *I-V, C-V, XRD* dan *parameter S* untuk pencirian *DC* dan *RF*. Kajian menunjukkan bahawa dwilapisan Platinum/Paladium (Pt/Pd) adalah pilihan terbaik untuk sentuhan logam schottky cirian *DC* berbanding dengan logam Schottky lain berdasarkan formasi lowongan Ga pada kawasan antaramuka Schottky yang menyebabkan kebocoran arus pincang belakang yang lebih rendah, kestabilan terma yang lebih baik pada suhu tinggi sehingga suhu 800°C. Respons frekuensi dari simulasi logam Schottky

berperilaku seperti penapis laluan tinggi manakala sentuhan yang di fabrikasi bersifat seperti penapis takik (impedan maksimum pada frekuensi resonan) disebabkan oleh kapasitan sesat dan kerintangan siri (kesan kulit). Pada umumnya, Pt/Pd menunjukkan kehilangan penyisipan yang lebih rendah berbanding dengan logam Schottky yang lain pada cirian *RF* manakala Al/Ti sebagai sentuhan ohmik menunjukkan peningkatan cirian garis lurus *IV* disebabkan oleh formasi lapisan antaramuka TiN dan peningkatan kestabilan terma sehingga 900°C disebabkan oleh formasi aloi Al dan Ti.

Sifat terma diod schottky n-GaN telah dikaji pada suhu bilik sehingga pada suhu 900°C. Kajian menunjukkan bahawa penurunan nilai voltan runtuh dan peningkatan dalam kehilangan penyisipan pada peningkatan suhu adalah disebabkan oleh penorowongan berbantukan fonon dan penjanaan elektron bebas pada sepanjang kawasan sentuhan.

Untuk kajian berkaitan luas kawasan sentuhan Schottky, simulasi dan fabrikasi sentuhan Schottky, pelbagai panjang, dari sub-mikrometer (0.5µm) sehingga micrometer (4µm). Sentuhan Schottky yang lebih panjang telah mengurangkan nilai voltan runtuh *DC* dan meningkan nilai kehilangan sisipan *RF* akibat peningkatan kapasitan simpang berhampiran kawasan sentuhan Schottky. Kaedah “penanaman semula” telah berjaya dilaksanakan dalam usaha mengurangkan kehilangan parasitik tersebut.

Dalam usaha memperbaiki kebocoran arus sekitar tebing kawasan berlogam diod schottky n-GaN, teknik penamatan tebing logam bertindih telah disimulasikan. Arus pincang depan meningkat bermula dari filem nipis oksida (0.001 µm) sehingga ke suatu had pada panjang (X_0) 1.5 µm plat medan bertindih. Perbaikan ini mungkin disebabkan oleh formasi lapisan akumulasi berkerintangan rendah dalam

semikonduktor. Akhir sekali, seperti yang dijangkakan, voltan runtuh meningkat seiring dengan ketebalan lapisan oksida sehingga suatu had disebabkan oleh taburan medan elektrik di dalam semikonduktor.

DC AND RF CHARACTERIZATION OF n-GaN SCHOTTKY DIODE FOR MICROWAVE APPLICATION

ABSTRACT

Gallium nitride is a promising wide bandgap semiconductor material for high-power, high temperature and high frequency device applications. However, there are still a number of factors that are limiting the material to reach a satisfactory device performance. Among them the most important and critical factors are the reverse leakage current, series resistance, junction capacitance and thermal stability that limits Schottky diode performance on gallium nitride for Direct Current (DC) and Radio Frequency (RF) characteristics. To overcome these limitations we studied the influence of metal contact, contact area, thermal behavior and edge termination on DC and RF characteristics of n-GaN Schottky diode by simulation and fabrication approach.

For metal contact study we simulate and fabricate n-GaN Schottky diode using wide variety of single metal Platinum(Pt), Nickel(Ni), Palladium (Pd), and bilayer Schottky metals Platinum/Palladium(Pt/Pd), Platinum/Nickel(Pt/Ni), and Platinum/Titanium(Pt/Ti) annealed from room temperature up to 800ºC while Aluminum/Titanium (Al/Ti) for ohmic contact annealed from room temperature up to 900ºC, to study the reverse leakage current, thermal stability and insertion losses using various techniques such as current-voltage (I-V),capacitance-voltage (C-V), Scanning electron microscope (SEM),X-ray diffraction (XRD) and Scattering parameters (S-parameters) for DC and RF characteristics. Studies shows that Platinum/Palladium (Pt/Pd) bilayer Schottky metal are the best choice for DC characteristics among other Schottky metals due to Ga vacancies formation at the

Schottky interface area showing lower reverse leakage current, better thermal stability up to 800ºC at elevated temperatures. The frequency response of simulated Schottky metal behave as high pass filter while fabricated contact behaves like notch filter (maximum impedance at resonant frequency) due to stray capacitance and series resistance (skin effect). In general, Pt/Pd bilayer shows lower insertion loss compared to other Schottky metal for RF characteristics while Al/Ti as ohmic contact shows improved linear (I-V) characteristics due to TiN interfacial layer formation and high thermal stability up to 900ºC due to Al and Ti alloys formation.

Thermal behaviors of n-GaN Schottky diode were studied from room temperature to 900ºC. The Study shows that breakdown voltage reduced and insertion loss increases with temperature increase due to phonon assisted tunneling and free electron generation across the junction contact area.

For Schottky contact area, we simulate Schottky contact length, varies from submicron (0.5µm) to micrometer (4µm). The increase in Schottky contact length decreases DC (breakdown voltage) and RF (insertion loss increases) due to increase in junction capacitance near the Schottky contact area. The de-embedding techniques have been successfully implemented to reduce these parasitic losses.

In order to further improve the leakage current around the edge of the metalised area, metal overlaps edge termination techniques have been simulated. The forward current improved for thinner oxide (0.001 µm) film up to certain limit of field plate overlap length (X_0) 1.5 µm. This improvement is likely due to formation of low resistivity accumulation layer in semiconductor. Finally, as expected, the breakdown voltage increased with terminated oxide at certain limit of oxide thickness due to electric field distribution inside semiconductor.

CHAPTER 1

INTRODUCTION

1.1 Introduction to Schottky diode

For high-speed applications of electronic circuits, one of the problems exhibited by semiconductor devices is a phenomenon called charge storage. This term refers to the fact that both free electrons and holes tend to accumulate inside a semiconductor crystal while it is conducting, and must be removed before the semiconductor device is turn off. This is not a major problem with free electrons, as they have high mobility (low effective mass) and will rapidly leave the semiconductor device. However, holes will pose a problem due to low mobility (high effective mass). They must be filled more gradually by electrons jumping from valence band to conduction band. Thus, it takes time for a semiconductor device to completely stop conducting. This problem is even worse for a transistor in saturation, since by definition the base region has an excess of minority carriers, which tend to promote conduction even when the external drive is removed (Bigelow, 2007).

The solution is to design a semiconductor diode with no p-type semiconductor region, therefore no holes as current carriers. Such a diode, known as a Schottky barrier diode or Schottky diode (named after German physicist Walter H. Schottky). Schottky diodes are known as majority carrier devices; a majority carrier device only utilizes one charge carrier, compared with a P-N diode, which relies on random recombination of electron-hole pairs, which limits the switching speed because of the charge storage effect. The lower forward resistance and junction capacitance are the most important advantages of the Schottky barrier diode. The lower forward resistance leading to lower levels of power loss compared to ordinary

PN junction diodes makes Schottky diode useful in power application. The lower junction capacitance generated by Schottky diodes makes them especially suitable as a radio frequency (RF) application such as microwave receiver detector and mixers.

There are many forms of Schottky diodes available; a planar Schottky diode is formed when a high work function metal layer is deposited directly onto a low doped n-semiconductor region. When metal and semiconductor are brought into contact with each other, the potential (work function) difference between metal and low doped semiconductor gives rise to a barrier height that the electrons have to overcome for current to flow. Applying a forward bias lowers the barrier, allowing current to flow while reverse bias increases the barrier's height, preventing current flow. The metal on the low-doped semiconductor is the anode (Schottky contact) and the metal which contacted through high doping substrate to the semiconductor material is the cathode (ohmic contact). Not all metal-semiconductor junction are Schottky barrier diode, it is depends on the metals work function, the bandgap of the intrinsic semiconductor, and the type and concentration of dopants in the semiconductor.

Schottky diodes has many application in today's high technology electronics scene such as photodetectors, metal gate field-effect transistors (MESFETs), modulation-doped field-effect transistors (Modulation-doped FET (MODFETS) or High Electron Mobility Transistors (HEMTs)), microwave mixers, RF attenuators, rectifiers, and various integrated circuits, it is actually one of the oldest semiconductor devices in existence. As a metal -semiconductor device, its application can be traced before 1900, where crystal detector, cat's whisker detector and the like were all effectively Schottky diodes. In 1938, Walter Schottky created a theory of rectifying behavior of a metal-semiconductor contact later built Schottky

barrier diodes on the basis of this theory (Schottky, 2002). The Schottky barrier diode is actually a variation of the point-contact diode in which the metal semiconductor junction is a surface rather than a point contact. The point contact diode were found to be very unreliable requiring frequent repositioning of the wire to ensure satisfactory operation, and they were subsequently replaced by a technique in which metal was vacuum deposited. The evaporation of metal films in a high vacuum system produced contacts which were more stable and reproducible than point–contacts. The point contact diode usually has poor forward and reverse I-V characteristics compared with Schottky diode due to large series resistance and leakage current. The advantage of point-contact diode is its small contact area which can give very small capacitance a desirable feature for microwave application.

The large contact area or barrier between the metal and the low doped semiconductor in the Schottky barrier diode provides some advantages over the point-contact diode (Fnrf, 2004). Besides these advantages of large contact area, or metal contact barrier, it shows large leakage current, series resistance and junction capacitance which limits the DC and RF performance of Schottky diodes for microwave application (Guo *et al*. 2001). High reverse leakage current due to defect states around the edge of the metalised area plays a significant role on the DC performance of Schottky diode (Harris *et al.* 1999).

To overcome these two terminal limitations, some studies have been published on important areas of Schottky diode such as, metal contact on n-GaN (Monroy *et al.* 2006, Liu and Lau 1998, Schmitz *et al.* 1997), contact area on SiC (Schoen *et al.*1998 and Singh *et al.* 1997) and edge termination on SiC (Chyi *et al.* 1999, Bandit *et al.* 1999, Tarplee *et al.* 2001) to optimize the DC performance of

Schottky diode but so far no research published the RF performance of n-GaN Schottky diode for microwave application.

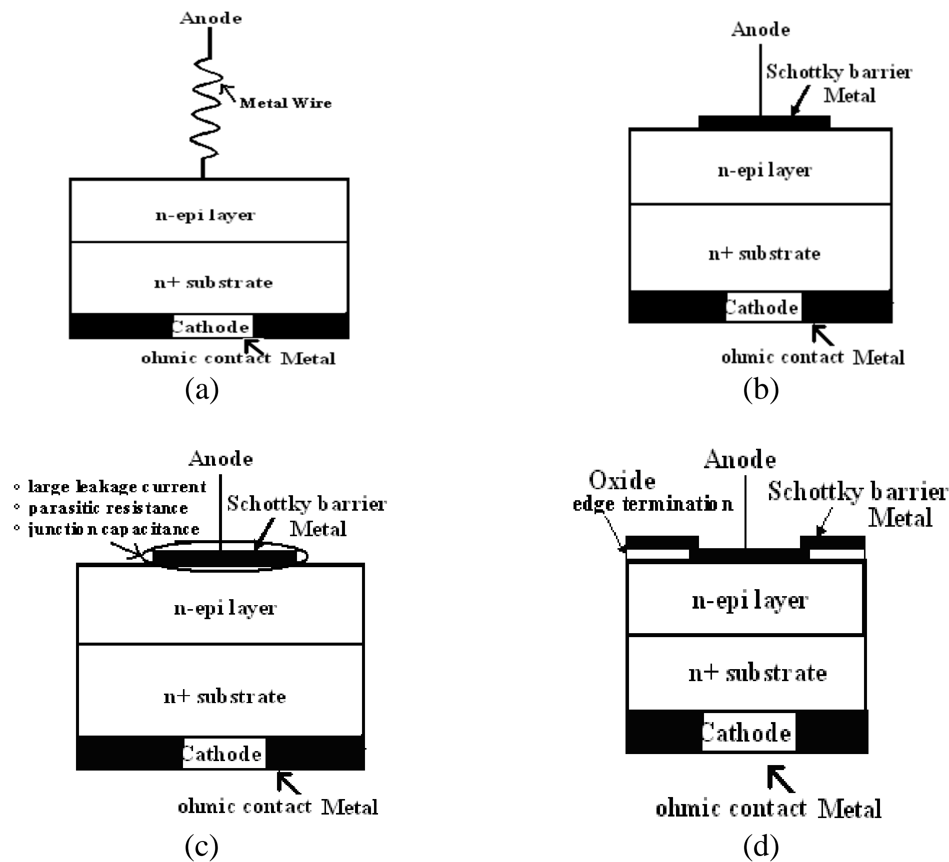

Figure 1.1: (a) Point contact diode. (b) Planar Schottky barrier diode.
(c) Problems in Schottky diode. (d) Edge-termination Schottky diode.
(Fnrf, 2004 & Adrio communication, 2005)

1.2 Ideal material properties for high power and high frequency application

Material properties vary widely in semiconductors and only certain materials are suitable for high power and high frequency devices. In Table 1.1, there are a number of semiconductor material properties that affect the performance of a high speed and high power devices. These include the bandgap, critical (breakdown) electric field, and thermal conductivity, the saturated electron velocity, electron and hole transport properties, strongly influence the DC and RF characteristics of semiconductor devices.

The large bandgaps of 3.4 eV for GaN and 3.2 eV for 4H-SiC give these materials a high temperature performance advantage over Si and GaAs. The wider bandgap is the higher temperature at which power device can operate and can withstand more heat and radiation without losing their electrical characteristics.

The critical (breakdown) electric fields of GaN and SiC have 3.5 MV/cm, five times that of Si or GaAs. This critical, or breakdown field of a material is possibly the most important material parameter for design of a high power density device, as it determines the highest operating voltage for a given device design.

The thermal conductivity of SiC of 4.9 W/cm-K is three times that of Si and ten times that of GaAs or sapphire and, as such, is a tremendous advantage for SiC-based devices. Since GaN-based devices are grown on both sapphire and SiC substrates at the present time, the limiting thermal conductivity for these devices depends on the choice of substrate.

SiC has a measured saturated electron velocity of 2.2×10^{7} cm/second, twice which of Si or GaAs, and GaN has an electron velocity of 1.5×10^{7}cm/second, still significantly higher than that of Si or GaAs.

SiC and GaN have electron mobilities of 800 to 1000 cm^2/V-sec in nominally undoped material. These values are much less than the 1350 cm^2/V-sec electron mobility of silicon, let alone the 6000 cm^2/V-sec electron mobility of GaAs. The hole mobility in both SiC and GaN is very low, 120 ~ 300 cm^2/V-sec. The low value for hole mobility severely limits the use of p-type SiC and GaN in RF transistors that are intended for operation above about 1 GHz.

In general, GaN may be regarded as the material of choice for high power and high frequency application due to the advantages discussed above and summary in Table 1.2.

Table 1.1: Material properties of common semiconductors. (Golio, 2003)

Property	Units	Silicon	GaAs	4H-SiC	GaN
Bandgap	Ev	1.11	1.43	3.2	3.4
Breakdown field	V/cm	7×10^5	7×10^5	35×10^5	35×10^5
Saturation velocity	cm/sec	1×10^7	1×10^7	2×10^7	1.5×10^7
Saturation field	V/cm	8×10^3	3×10^3	25×10^3	15×10^3
Thermal conductivity	W/cm-K	1.5	0.46	4.9	1.7/substrate
Electron mobility	Cm^2/V-sec	1350	6000	800	1000
Hole mobility	Cm^2/V-sec	450	330	120	300

Table1.2: GaN properties for high power and high frequency. (Borges, 2001)

Property	Si	GaAs	SiC	GaN
Suitability for High Power	Medium	Low	High	High
Suitability for High Frequencies	Low	High	Medium	High
HEMT structures	No	Yes	No	Yes
Low Cost Substrates	Yes	No	No	Yes

1.3 Issues in GaN Schottky diode

GaN shows wide application in optical and electronic devices, such as high-temperature, high power and high frequency transistors like MESFETs and HEMTs. Although, GaN shows superior properties as compared to other semiconductor for high power and high frequency application explained in previous section, there are still a lot of issues must be investigated and resolved in order to obtain the robust material properties of GaN (Nanjo *et al.* 2004). The detailed discussion of these issues will be described in Chapter 2 literature review.

One of the serious problems with GaN Schottky diode is a large voltage drop across the GaN/ metal interface at ohmic contacts, which leads to poor device performance and reliability. In order to improve these, the development of low resistance ohmic contacts to both n- and p-GaN is essential (Pal and Sugino, 2000).

Low resistance ohmic contacts for GaN are particularly challenging, as compared to the other well studied III-V compounds (GaAs and InP) because of its large band gap. Although the nitrides, GaN, AlN, and InN, show great potential for optical and electrical devices, there still remains much more works to be done in obtaining ohmic contacts with small specific resistivities (Lin *et al.* 1994, Liu and Lau, 1998).

One of these issues is the GaN -based Schottky interfaces are known to suffer from unusually large leakage currents under reverse bias. Reducing the relatively high gate leakage current is one of the key issues. Excess leakage currents through a Schottky gate strongly affects not only gate-control and power consumption but also the noise performance and breakdown voltage in GaN-based FET devices as recently pointed out (As *et al.* 2006, Oyama *et al.* 2002, Miller *et al*. 2003). Therefore, a high quality Schottky contact to GaN must be found, in order to reduce the reverse-biased leakage current in Schottky diodes (Miura *et al.* 2004).

GaN has been considerable interests for MESFETs, MOSFETs and MODFETs. For these applications, high quality ohmic and Schottky contacts have been key factors in improving performance and reliability. The operating condition of these applications, often involves elevated temperature. Therefore, it is vital to understand the behaviour of metal contacts and relevant degradation mechanism to GaN at high temperature (Monroy *et al.* 2006 and Wang *et al.* 2003).

GaN Schottky diode demands not only high frequency operation but also thermal stability. The heat generated during power operation may significantly increase the device temperature which degrades device performance drastically. Therefore, it is important to understand the operation mechanism at higher temperature (Ye *et al.* 2006).

One of the more serious issues is the large series resistance and junction capacitance across the Schottky metal contact area which limits the high power and high frequency performance of GaN Schottky diode for microwave application (Baliga *et al.* 1996). Control of these parasites is a key issue in the development of advanced transistors. The Schottky metal contact area is an important design consideration because it directly affects the breakdown voltage and forward bias current conduction capabilities of GaN Schottky diode (Pearton *et al.* 2001).

Edge termination techniques such as guard rings, metal overlap on an oxide layer and mesa etc, are generally adopted for high voltage devices, in order to relief the electric field enhancement around the contact periphery and thus yield a near ideal planar breakdown voltages (Zhang and Sudarshan, 2001). However, there has been little effort employing in edge termination techniques in GaN Schottky diodes (Pearton *et al*. 2000, Zhang *et al.* 2002).

1.4 Research objectives

The objective of this research is to address issues on GaN Schottky diode discussed in previous section, specifically on metal contact, thermal behavior, Schottky contact area and edge termination. To achieve this objective, this work will study the leakage current, thermal stability, series resistance and parasitic capacitance, insertion losses (S_{21}dB) that limit the DC and RF characteristics for microwave application.

Even though several studies on wideband gap semiconductor such as SiC and GaN in improvement of DC characteristics were already published as far as we aware, there are no published work on RF characteristics. Detail of this method will be described in detail in the thesis.

To study metal contact properties, we simulate and fabricate various high work function single Schottky metals (Pt, Ni, Pd) and bilayer Schottky metal (Pt/Ti, Pt/Pd and Pt/Ni) annealed from room temperature up to 800°C under N_2 ambient. We expect that Pt/Pd bilayer metal to exhibit lower reverse leakage current, better surface morphology, greater thermal stability up to 800°C under N_2 ambient compared to other single and bilayer Schottky metal contacts due to Ga vacancies formation at the Schottky interface area. Frequency response of Schottky metal contact behaves like notch filter (maximum impedance at resonant frequency) whereas Pt/Pd shows lower insertion loss with temperature increase up to 800°C compared to other Schottky metal contact. Standard Al/Ti metallization scheme will be used as ohmic contact since it shows linear (I-V), lower capacitance, most probably due to TiN interfacial layer formation and high thermal stability annealed up to 900°C under N_2 ambient due to reaction of Al and Ti intermetallic alloys.

Thermal behavior of n-GaN Schottky diode at various temperatures from (300 K to 900 K) is studied by simulation and fabrication. We expect, as the temperature increases, breakdown voltage decreases showing negative temperature coefficient might be due to phonon-assisted tunneling of electrons from electronic states/traps. While for RF behavior, insertion loss increase and resonant frequency decreases with temperature due to free electron carrier generation across Schottky interface area. This information is vital in determining the thermal limitation on device performance.

Schottky contact area varies from submicron to micron will be simulated and fabricated. The increase in Schottky contact length is expected to decreases breakdown voltage for DC analysis and increases the resonant frequency peak for RF

characteristics due to increase in junction capacitance near the Schottky contact area. The de-embedding techniques will be implemented to reduce the parasitic losses.

And, finally metal overlap edge termination techniques on n-GaN will be simulated. Forward current is expected to improve due to metal overlap edge termination techniques for thinner oxide, up to certain limit of field plate length. Furthermore, ramp oxide edge techniques should improve the forward bias characteristics as compared to the terminated oxide diodes and the breakdown voltage is expected to increase with terminated oxide diode up to certain limit of oxide thickness.

At the end of this work, we will established an optimized GaN Schottky device, suitable for high power and high frequency applications.

1.5 Thesis organization

The content of this thesis is divided into two sections: First section, of thesis describes the overview, theoretical DC and RF parameter extraction, simulation tools and models, simulated results of n-GaN Schottky diode. Second section, describes the fabrication process, results and discussion of fabricated n-GaN Schottky diode. Finally, conclusion of simulated and fabricated n-GaN Schottky diode DC and RF characteristics for microwave application.

Chapter 2 encompasses an overview of the GaN Schottky diode important issues such as metal contact, thermal behavior, contact area and edge termination technique on DC and RF characteristics for microwave application.

Chapter 3 presents, theoretical and detailed study of DC and RF parameter extraction of GaN Schottky diode. Chapter 4 presents, simulation tools and models.

Chapter 5 simulated results of n-GaN Schottky diode important areas such as metal contact, thermal behavior, contact area, and edge termination technique for DC and RF characteristics.

Chapter 6 presents, fabrication process of GaN Schottky diode that includes mesa mask step by step fabrication process. Chapter 7 provides, results and discussions of fabricated n-GaN Schottky diode important issues such as metal contact, thermal behavior and de-embedding technique.

Finally, Chapter 8 presents summary of results obtained from simulation and fabrication of n-GaN Schottky diode on important issues such as metal contact, thermal behavior, Schottky contact area and edge termination. A few suggestions for future research are also included.

CHAPTER 2

OVERVIEW OF GaN SCHOTTKY DIODE

2.0 Introduction

In the Schottky diode design process many important decisions must be made to assemble the materials into a device that meets the desired DC and RF characteristics for microwave application. Schoen *et al.* (1998) the main design variables that affect the Schottky diode performance for DC and RF characteristics are metal contact, thermal behavior, contact area and selection of an edge termination technique which will be described briefly in this chapter.

2.1 Metal-contact technology

The metal-semiconductor (MS) contact plays a very important role in all the solid-state devices. Two types of contacts are often used: ohmic contacts and rectifying or Schottky contacts. A Schottky barrier contact exhibits an asymmetrical current– voltage (*I*–*V*) characteristic when the polarity of a bias voltage applied to the metal–semiconductor contacts is changed. The ohmic contact, on the other hand, shows a linear *I*–*V* characteristic regardless of the polarity of the external bias voltage (Fig 2.1). A good ohmic contact is referred to the case that the voltage drop across a metal–semiconductor contact is negligible compared to that of the bulk semiconductor material.

An ideal metal-semiconductor contact has the following properties:

- The metal and semiconductor are assumed to be intimate contact on an atomic scale, with no layers of any type (such as oxide) between the components.
- There is no inter-diffusion or inter-mixing of the metal and semiconductor

- There are no adsorbed impurities or surface charges at the MS interface.

Indeed, real contacts are neither perfectly ohmic nor perfectly rectifying. If due care is taken in the fabrication, however, good approximations of the ideal can be achieved. The overall conclusion is that an ideal MS contact formed from a metal and an n-type semiconductor will be a rectifying contact if metal work function (ϕ_m) greater than semiconductor work function (ϕ_s) i.e ($\phi_m > \phi_s$) and an ohmic-like contact if $\phi_m < \phi_s$. Parallel arguments applied to an ideal MS contact formed from a metal and a p-type semiconductor lead to the conclusion that the contact will be rectifying if $\phi_m < \phi_s$ and ohmic-like if $\phi_m > \phi_s$. These conclusions are summarized in Table 2.1.

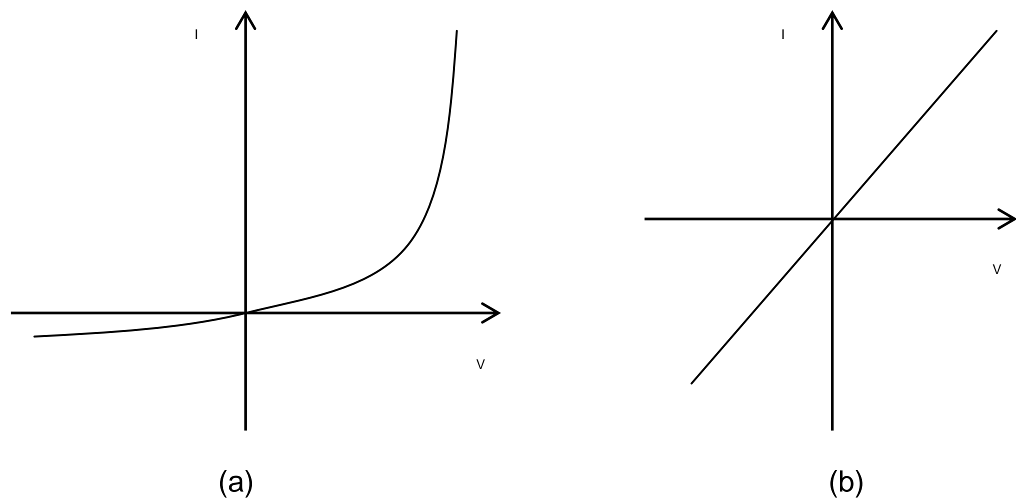

Figure 2.1: Characteristics of (a) rectifying (b) linear or ohmic I-V.

Table 2.1: Electrical nature of Ideal MS contacts. (Pierret, 1996)

	n-type semiconductor	p-type semiconductor
$\phi_m > \phi_s$	Rectifying	Ohmic
$\phi_m < \phi_s$	Ohmic	Rectifying

2.1.1Energy band diagram metal/semiconductor and Schottky barrier formation

Figure 2.2 shows the schematic energy band diagrams for a metal/n-type semiconductor system before and after contact and under various conditions.

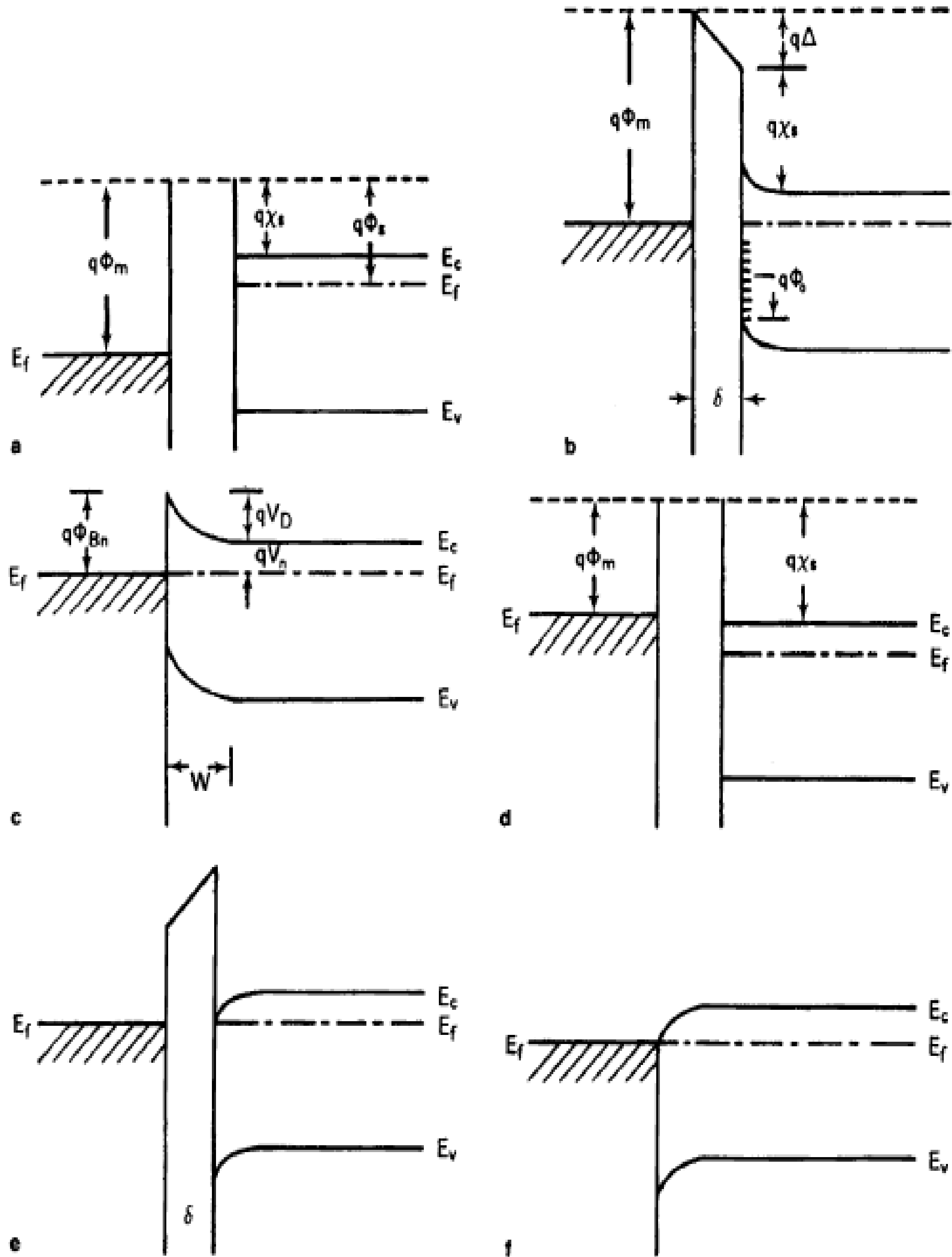

Figure 2.2: Energy band diagrams for an ideal metal/n-type semiconductor contact. (a) to (c) $\Phi_m > \Phi_s$: (a) before contact, (b) in contact with a small air gap and interface states, (c) in intimate contact (rectifying contact), with no interface states: (d) to (f) $\Phi_m < \Phi_s$, (d) before contact, (e) in contact with a small air gap, and (f) in intimate contact (ohmic contact).(Sheng, 2005)

When a metal comes into contact with a semiconductor Schottky barrier may form. Fig. 2.2(a) is the energy band diagram for n-type semiconductor with a work function less than that of the metal ($\phi_m > \phi_s$). Fig.2.2(c) we suppose that there is no surface states present, if the metal and semiconductor are connected each other, electron pass from the semiconductor into the metal and two Fermi levels are forced into coincidence. The energies of electrons at rest outside the surface of two solids are no longer the same, and there is an electric field in the gap directed from right to left. There must be a negative charge on the surface of the metal balanced by a positive charge in the semiconductor. Since the semiconductor is n-type, the positive charge will be provided by conduction electrons receding from the surface, leaving uncompensated positive donor ions in a region depleted of electrons. The uncompensated donors occupy a layer of appreciable thickness *W*, comparable to width of the depletion region in a p-n junction, and the bands in the semiconductor are bent upwards. The difference V_i between the electrostatic potential outside the surfaces of the metal and semiconductor is given by:

$$V_i = \delta\varepsilon_i \qquad (1.1)$$

where δ is their separation and ε_i the field in the gap.

If the metal and semiconductor approach each other, V_i must tend to zero if ε_i is remain finite and, when they finally touch, the barrier due to vacuum disappears altogether and we are left with an ideal metal-semiconductor contact. It is clear from the fact that V_i tends to zero that the height of the barrier Φ_{Bn} measured relative to the Fermi level is given by:

$$\Phi_{\mathrm{Bn}} = \Phi_{\mathrm{m}} - \chi_{\mathrm{s}} \qquad (1.2)$$

where Φ_{m} is the metal work function, χ_{s} semiconductor electron affinity.

That was first stated implicitly by Mott (1938) and will be referred as the Schottky-Mott limit. But experimentally it is found that the barrier height may be almost independent of the choice of metal. An explanation of this weak dependence was put forward by Bardeen (1947), who suggested that the discrepancy may be due to the effect of surface states or interface states. Fig. 2.2(b) suppose that the metal and semiconductor remain separated by a thin insulating layer and that there is a continuous distribution of surface states present at the interface between semiconductor and the insulator, characterized by a neutral level Φ_0. The occupancy of the surface states will be below or up is determined by the Fermi level. If the Φ_0 happens to be below E_F, this means that the width W of the depletion region will be correspondingly increased, and the amount of band bending (barrier height Φ_{Bn}) will also be increased and Φ_0 will be pushed up towards E_F. It is usual in the literature to measure Φ_0 from top of the valence band, in which case the barrier height will be given by:

$$\Phi_{Bn} \approx E_g - \Phi_0 \tag{1.3}$$

This will be called the Bardeen limit. The barrier height is said to be 'pinned' by the high density of surface states.

Fig. 2.2 (f) shows metal work function is less than semiconductor work function ($\phi_m < \phi_s$).Clearly, if such contact is biased so that electron flow from the semiconductor to the metal, they encounter no barrier. Such a contact is termed an ohmic contact. This type of contact has a sufficiently low resistance for the current to be determined by the resistance of the bulk semiconductor rather than by the properties of the contact. For a metal/p-type semiconductor contact, the opposite behavior results.

2.1.2 Conduction mechanism for metal/semiconductor contacts

The three primary mechanisms govern current transport across a metal-to-semiconductor interface: thermionic emission, field emission and thermionic-field emission (Schroder, 1998 and Schen *et al*. 1992) shows in Fig 2.3. They differ mainly by the interface potential barrier height and width as determined by the work function of the metal, the semiconductor electron affinity and the semiconductor doping concentration near the interface.

- Thermionic emission is important when both the barrier and doping concentration are low. In thermionic emission, electron thermally excited to energies above the barrier, pass directly over it. As a result, contact resistance where thermionic emission dominates depends strongly on temperature.
- Thermionic field emission is important when both barrier and doping concentration are moderate. In thermionic-field emission, electrons are thermally excited part way up the potential barrier at which point they tunnel the rest of the way through. Thermionic-field emission is moderately temperature dependent. Typically, some sort of thermionic-field emission is the most likely transport mechanism.
- Field emission is important when both the barrier and doping concentration are high. A high doping concentration reduces the width of the carrier depletion region near the semiconductor surface. This in turn produces a thin barrier that electron tunnel through directly. A field emission is only weakly dependent on temperature.

Conduction mechanism for GaN is normally dominated by thermionic emission mode.

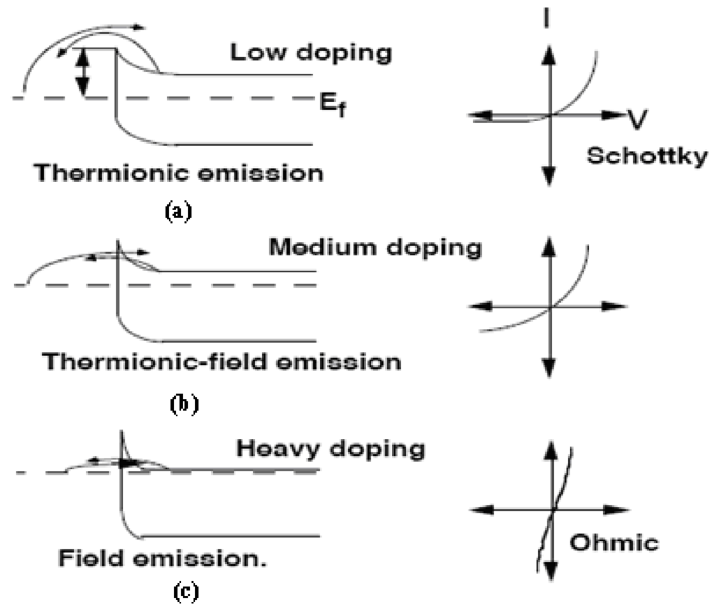

Figure 2.3: Conduction mechanism for metal/n-semiconductor contacts as a function of the barrier height and width, (a) Thermionic emission: (b) Thermionic field emission: (c) field emission. (Schroder, 1998 and Schen *et al.* 1992)

2.1.3 Current conduction mechanism in metal/semiconductor

The energy band diagrams and current components for an ideal metal/n-type semiconductor under zero-bias, forward-bias, and reverse-bias conditions are shown in Fig. 2.4 (a), (b), and (c), respectively. The potential barrier for electrons moving from the semiconductor side to the metal side is designated as (V_D), while the potential barrier for electrons moving from the metal side to the semiconductor side is defined as (Φ_{Bn}).

If a forward-bias voltage (V_a) is applied to the Schottky diode, then the potential barrier on the semiconductor side of the diode is reduced to $V_D - V_a$, as is shown in Fig.2.4 (b). It is noted that the barrier height remains relatively unaffected by the applied bias voltage or the doping density of the semiconductor. Thus, the current flow from the semiconductor to the metal increases dramatically under forward-bias condition, while the current flow from the metal to the semiconductor

remains essentially the same. Under forward-bias condition, the net current flow is controlled by the electron current flow from the semiconductor to the metal.

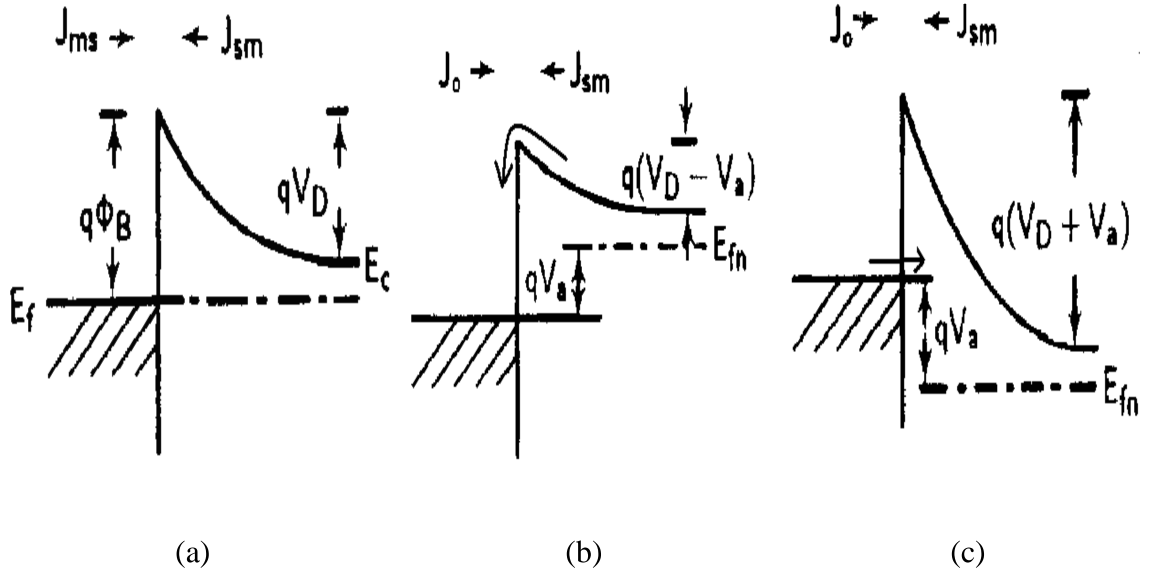

Figure 2.4: Energy band diagrams and current components for Schottky barrier diode under (a) Zero bias (b) forward bias (c) reverse bias. (Sheng, 2005)

Under reverse-bias condition, the potential barrier on the semiconductor side increases to $V_D + V_a$, and the current flow from the semiconductor to the metal becomes negligibly small compared to the current flow from the metal to the semiconductor. Thus, the net current flow under reverse bias condition is controlled by the thermionic emission from the metal to the semiconductor, as is shown in Fig.2.4 (c).

The thermionic emission model developed by Bethe and the diffusion model developed by Schottky are the most widely used physical models for predicting the *I–V* characteristics of a Schottky barrier diode. The current flow from metal to semiconductor side in thermal equilibrium $Va = 0$

$$J_{ms} = -J_{sm} = -J_O \tag{2.1}$$

While

$$J_{sm} = A^*T^2 \exp\left(\frac{-q\Phi_B}{k_B T}\right)\left[\exp\left(\frac{qv_a}{k_B T}\right)\right] \tag{2.2}$$

Where

$$J_0 = A^*T^2 \exp\left(\frac{-q\Phi_B}{k_B T}\right) \tag{2.3}$$

where A^* is effective Richardson constant $A^* = 26A/cm^2K^2$ for n-GaN, Φ_B is the barrier height.

Thus, the total current flow under forward-bias condition is equal to

$$J = J_{sm} + J_{ms} = J_0\left[\exp\left(\frac{qv_a}{k_B T}\right) - 1\right] \tag{2.4}$$

Equation (2.4) is the well-known Schottky diode equation, which predicts an exponential dependence of the current density on both the temperature and applied bias voltage. Since the saturation current density (J_0) depends exponentially on the barrier height, a large barrier height is needed in order to reduce the value of J_0 in a Schottky diode.

2.2 Metal-GaN contact technology

The first parameter to be discussed for a metal –semiconductor contact is the ohmic contact. The ohmic contact is commonly referred to as the backside contact. It provides a contact area for the cathode. In the selection of a metal for this contact, it is important to choose a metal with a low work function and low series resistance (Saxena and Steckl, 1998). However, in order to prevent the ohmic contact from becoming an extra, unwanted Schottky contact, the metal must alloy well to the substrate. This is done by a process called the contact anneal which is a high temperature annealing process. Since the ohmic contact anneal is the highest

temperature process, it must be done prior to Schottky contact formation. In the following sections we examine the recent advances in metal-GaN contact technology to shed light on some of the critical technological issues.

2.3Ohmic contact to n-GaN

As the GaN device technology advances, more stringent requirements are needed for the fabrication of metal contacts with very low resistance, good thermal stability and flat surface morphology. It is widely known that parasitic resistances, in the form of contact resistance, significantly affect the overall performance of the electronic and optical devices (Lin *et al*. 1994).

The large voltage drop across the semiconductor/metal interface at the ohmic contacts will seriously lead to the loss of device performance and reliability. Therefore, high quality and thermally stable contacts to GaN-based materials are essential for the fabrication of reliable, efficient, high performance devices and circuits.

In an earlier attempt to achieve ohmic contacts on n-GaN, Foresi *et al.* (1993) used Al and Au contacts. Most of the ohmic contacts investigated so far fall into this category which includes schemes such as, the Al-only contact, Ti–only contact, Al/Ti bilayer contact and modifications of the Al/Ti bilayer contacts. The oxidation of Al during thermal annealing is difficult to avoid in practice. This can degrade the contacts significantly and the use of Al-GaN reaction for ohmic contacts may not be controllable and reproducible. Furthermore, the low melting point of Al (660 ºC) is not conducive to stable contacts. Therefore, Al only contacts are perhaps not applicable to GaN-based devices for high temperature and/or high power applications. The Ti has higher affinity to oxygen and is well known to be easily

oxidized even at room temperature. Therefore, Ti –only contacts are not applicable for reliable and high performance ohmic contacts in nitride devices.

Lin *et al.* (1994) have succeeded in obtaining extremely good ohmic contacts on n-type GaN layers grown on sapphire substrates utilizing Al/Ti metallization scheme. They were able to achieve specific contact resistivity (ρ_c) as low as 8×10^{-6} Ωcm^2 via conventional electron beam evaporation onto GaN substrate followed by thermally annealing at 900°C for 30s in an N_2 ambient. Ideally, upon thermal annealing, reactions between Ti and GaN should lead to the formation of ohmic contact. At the same time, reactions between Ti and Al should lead to the formation of a cap layer of intermatallic alloys Al_3Ti in particular. This cap layer should make the entire contact stable and reliable because Al_3Ti has higher resistance to oxidation than either Al or Ti, and a higher melting point than Al. The low specific contact resistivity obtained after thermal annealing at 900ºC for 30 s was believed due to the formation of a highly n-typed doped GaN layer and a thin TiN interfacial layer from the reactions between Ti and GaN, which is explained in next section. The TiN interfacial layer also lowers the effective barrier height and facilitating current conduction through the junction.

Fig. 2.5 shows the contact behavior of the Al/Ti contact. The contact became ohmic after thermal annealing at 600ºC for 20 s. The contact resistivity decreased sharply after annealing at 600ºC. In short, for the Al/Ti bilayer contacts, reactions between Ti (and / or Al) with GaN lead to the ohmic contact formation and reactions between Ti and Al to form Al_3Ti alloys lead to the thermal stability of the contacts. With an appropriate Al-to-Ti ratio and specific attention paid to ambient annealing gas to reduce oxidation, the Al/Ti bilayer contacts are robust ohmic contacts to n-

GaN. There is much room for further improvement for this contact scheme (Liu and Lau, 1998).

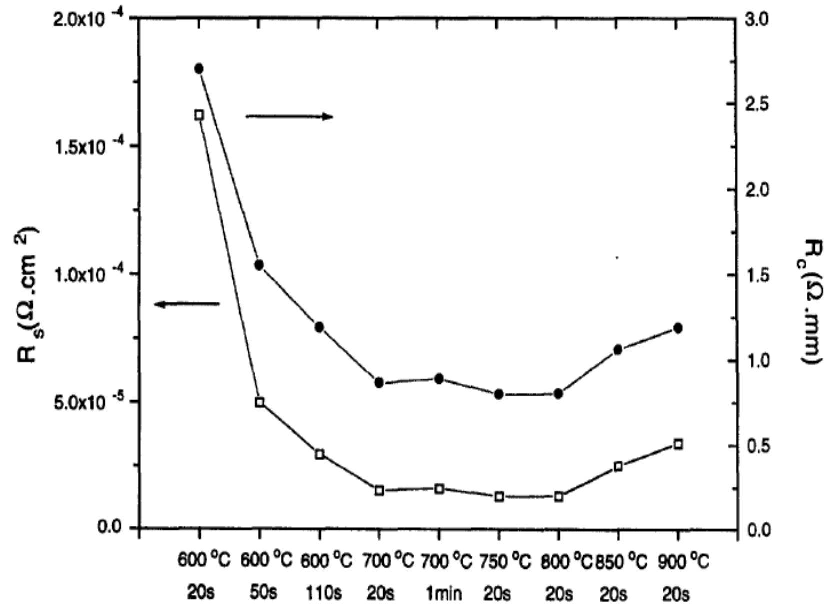

Figure 2.5: Ohmic behavior of Al/Ti contact on non-preannealed n-GaN samples as a function of annealing (Liu and Lau, 1998).

2.3.1 n-type conduction layer after thermal annealing

It was reported that the GaN crystal is unstable because of easy dissociation of nitrogen atoms from the GaN at high temperature (Thurmond and Logan, 1972, Madar *et al.* 1975, Lorentz and Binkowski, 1962, Karpinski *et al.* 1984, Groh *et al.* 1974, Vartuli *et al.* 1996) and are prone to reaction with GaN upon prolonged exposure to high temperatures (Schmitz *et al.* 1996, Venugopalan *et al.* 1997, Duxstad *et al.* 1996).

It was also reported that dissociation of nitrogen created nitrogen vacancies in the GaN and that vacancies acted as the donors (Maruska and Tietjen, 1969, Ilegemens and Montgomery, 1973, Jenkins and Dow, 1989, Neugebauer and Van de Walle, 1994). The nitrogen vacancies formed by the dissociation in to the heavily doped n-type layer, resulting in enhancement of electron tunneling rather than

thermionic emission through the metal/n-GaN. The conversion of the conduction type close to the n-GaN surface upon annealing at 700°C shown in Fig. 2.6. When the samples are annealed at high temperature, formation of n-type will give ohmic behavior. This conclusion is consistent with the result of the TiN_x contact, which provided ohmic behavior to n-type GaN and Schottky behavior to p-type GaN (Dimitriadis *et al.* 1999).

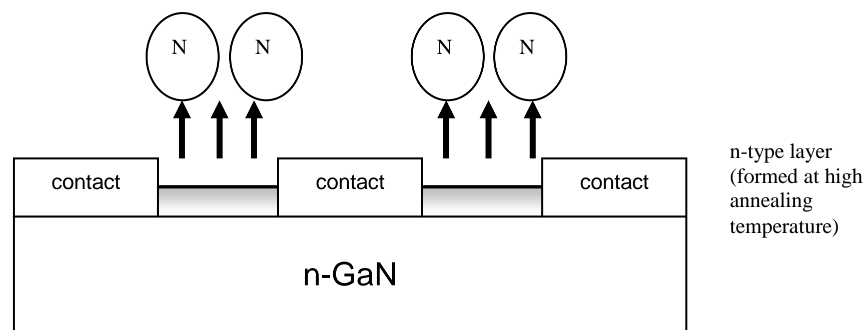

Figure 2.6: Schematic illustration of the n-GaN substrate annealed at 700°C.

2.4 Schottky contacts to n-GaN

Research into Schottky diodes on GaN has a particularly importance because extremely useful solid-state devices such as, FETs are not viable without a high quality Schottky contact. In other words, the development of a high quality Schottky contact is absolutely critical for the successful realization of GaN FETs in future (Suzue *et al.* 1996). The electrical improvement in AlGaN/GaN HEMTs reducing the relatively high gate leakage current is one of the key issues. The excess leakage has been reported to contribute to low-frequency noise as well as breakdown voltage of the device that determine their practicability to the power operation. Therefore, a high quality Schottky contacts to (Al)GaN must be found. In order to reduce the

reverse leakage current in Schottky diodes, metal possessing high work function chooses to maximize the effective Schottky barrier height against n-GaN or AlGaN/GaN HEMT. However, further improvement should be given to the Schottky contact to extract GaN robust material stability and to realize the long term integrity of GaN related devices. Therefore, various rare metals, alloys and multilayer systems have also been investigated and thermal annealing of the diodes in particular has been reported to be quite effective in some cases (Miura *et al.* 2004).

Due to the ionic character of the Ga-N bondings, the Fermi level at the nitride surface and at the metal-nitride interface should be unpinned: the barrier height should consequently depend on the work function or the electronegativity of the contacting metal (Wang *et al.* 2003). Schottky barrier heights of a variety of elemental metals including Au, Ti, Pd, Ni and Cr have been reported and summarized in Fig 2.7. We note that the Schottky barrier height (Φ_B) on n-GaN indeed varies with the metal work function.

The Schottky barrier height to n-GaN for a variety of elemental metals has been extensively studied. The reported barrier height increases monotonically, but does not scale proportionally with metal work function. The characteristics of Schottky barrier contacts are strongly influenced by the condition of the semiconductor prior to metallization. Ideally, metal/semiconductor interfaces should be inert, oxide and defect-free, atomically smooth and the metal epitaxial. It is also interesting to note that the Richardson's constant (A**) for GaN has been found to vary from 0.006 for Au to 64.7 $A.cm^{-2}. K^{-2}$ for Pt as compared to the theoretical value of 26.4 ($m^* \sim 0.22m_0$). In addition to this discrepancy, the following electrical characteristics are also often observed (Mohammad *et al.* 1996),